ELSEVIER

Chemical Geology 190 (2002) 91–112

CHEMICAL GEOLOGY
INCLUDING
ISOTOPE GEOSCIENCE

www.elsevier.com/locate/chemgeo

Variation in element release rate from different mineral size fractions from the B horizon of a granitic podzol

Mark E. Hodson *

Department of Soil Science, University of Reading, Reading, Berkshire, RG6 6DW, UK
Postgraduate Research Institute of Sedimentology, University of Reading, Reading, Berkshire, RG6 6DW, UK

Abstract

Far-from-equilibrium batch dissolution experiments were carried out on the 2000–500, 500–250, 250–53 and 53–2 μm size fractions of the mineral component of the B horizon of a granitic iron humus podzol after removal of organic matter and secondary precipitates. The different size fractions were mineralogically and chemically similar, the main minerals present being quartz, alkali and plagioclase feldspar, biotite and chlorite. Specific surface area increased with decreasing grain size. The measured element release rates decreased in the order 53–2 ⋙ 2000–500 > 500–250 > 250–53 μm. Surface area normalised element release rates from the 2000–500, 500–250 and 250–53 μm size fractions ($0.6–77 \times 10^{-14}$ mol/m^2/s) were intermediate between literature reported surface area normalised dissolution rates for monomineralic powders of feldspar ($0.1–0.01 \times 10^{-14}$ mol/m^2/s) and sheet silicates (100×10^{-14} mol/m^2/s) dissolving under similar conditions. Element release rates from the 53–2 μm fraction ($400–3000 \times 10^{-14}$ mol/m^2/s) were a factor of 4–30 larger than literature reported values for sheet silicates. The large element release rate of the 53–2 μm fraction means that, despite the small mass fraction of 53–2 μm sized particles present in the soil, dissolution of this fraction is the most important for element release into the soil. A theoretical model predicted similar (within a factor of <2) bulk element release rates for all the mineral powders if observed thicknesses of sheet silicate grains were used as input parameters. Decreasing element release rates with decreasing grain size were only predicted if the thickness of sheet silicates in the powders was held constant. A significantly larger release rate for the 53–2 μm fraction relative to the other size fractions was only predicted if either surface roughness was set several orders of magnitude higher for sheet silicates and several orders of magnitude lower for quartz and feldspars in the 53–2 μm fraction compared to the other size fractions or if the sheet silicate thickness input in the 53–2 μm fraction was set unrealistically low. It is therefore hypothesised that the reason for the unpredicted large release rate from the 52–3 μm size fraction is due to one or more of the following reasons: (1) the greater reactivity of the smaller particles due to surface free energy effects, (2) the lack of proportionality between the BET surface area used to normalise the release rates and the actual reactive surface area of the grains and, (3) the presence of traces quantities of reactive minerals which were undetected in the 53–2 μm fraction but were entirely absent in the coarser fractions.

Keywords: Mineral dissolution rates; Grain size; Reactive surface area

1. Introduction

The importance of mineral dissolution to a wide variety of natural phenomenon is reflected in the extensive literature concerning both laboratory and

* Current address: Department of Soil Science, Whiteknights, University of Reading, PO Box 233, Reading, Berkshire, RG6 6DW, UK. Tel.: +44-118-931-6557; fax: +44-118-931-6660.
E-mail address: m.e.hodson@reading.ac.uk (M.E. Hodson).

0009-2541/02/$ - see front matter © 2002 Elsevier Science B.V. All rights reserved.
PII: S0009-2541(02)00112-2

field studies dealing with this topic (e.g. White and Brantley, 1995 and references therein). For example, the dissolution of minerals in soil releases nutrients to the soil (Marschner, 1995) can neutralise acid rain (Hornung et al., 1995) and can play a role in the regulation of atmospheric CO_2 levels (Berner, 1995). In general, laboratory studies have concentrated on the dissolution of unweathered monomineralic powders whilst field based studies have dealt with the release of elements from soils, often using mass balance calculations to determine the dissolution rates of individual minerals.

In this study, different grain size fractions of the mineral component of the B horizon of a granitic soil were dissolved, after the removal of organic matter and secondary amorphous oxyhydroxides, in order to determine the relative importance of the dissolution of the different size fractions to the release of nutrients in soil. At least two scenarios can be envisaged. It could be the case that finer grain size fractions contain higher concentrations of unreactive, secondary reaction products thereby rendering them less reactive than coarser grain fractions. This is likely to be the case in soils with undisturbed bedrock as parent material. In contrast to this, the different size fractions of soils with glacial till as parent material are likely to have similar mineralogies due to the till containing finely ground bedrock. If dissolution rate is related to exposed mineral surface area, the relative importance of different size fractions will be determined by the relative dissolution rates of the different minerals present, the proportions of those minerals present, the surface area per unit mass of the size fraction (generally higher for fine fractions) and the relative proportions by mass of the different size fractions (generally higher for coarser fractions).

Thus, for a given soil, it is by no means clear whether dissolution of the finer or coarser mineral grain size fraction is the most important for element release. This study set out to investigate this question with respect to a granitic soil with a glacial till parent material.

2. Materials and methods

2.1. Soil preparation and characterisation

Soil from the B horizon of an iron-humus podzol with a parent material of till derived from a Devonian age biotite granite was collected from the Allt a'Mharciadh catchment in the Cairngorms, Scotland (see Bain et al., 1994 for a thorough description of this catchment). The soil was air-dried and dry sieved to a grain size of <2 mm. The soil was then dry sieved to yield 2000–500, 500–250, 250–53 and <53 μm size fractions. The <53 μm size fraction was separated into 53–2 and <2 μm size fractions by sedimentation. All but the <2 μm fraction were rewetted with deionised water and agitated using an ultrasonic probe in order to remove any fine particles adhering to grain surfaces. Next, the 2000–500, 500–250 and 250–53 μm grain size fractions were wet sieved using deionised water. The ultrasonically probed 53–2 μm fraction was again sedimented out. Finally, all the fractions were dried in an oven at 60 °C. The different fractions were weighed and the percentage by mass of each size fraction present in the soil was calculated (Table 1). Organic material was removed from the fractions by oxidation using hydrogen peroxide (Bock, 1979). Amorphous secondary precipitates were removed using a pH 3 acid ammonium oxalate extraction (McKeague and Day, 1966). Following removal of these components the size fractions were again agitated with an ultrasonic probe, sieved/sedimented out and dried at 60 °C. The specific surface area of the different fractions was determined by nitrogen gas adsorption and application of the BET isotherm (Brunauer et al. 1938) using a Coulter Surface Area analyser (Table 1). Repeat measurements over a period of several days indicate a precision of $\pm 5\%$ ($\pm 2 \times$ standard deviation on six repeat measurements for a powder of surface area 0.16 m^2/g) for these measurements.

Removal of organic matter and amorphous precipitates was carried out to allow comparison of the

Table 1
Percentage by mass of each size fraction present in the soil and specific surface area of the size fractions

Size fraction (μm)	Percentage of total grains by mass	Specific surface area (m^2/g)	Surface area (m^2) in 1 g of bulk mineral powder
2000–500	56	0.43	0.24
500–250	12	0.69	0.08
250–53	20	1.63	0.33
53–2	11	6.38	0.70
<2	1	67.10	0.67

dissolution rates of the mineral component of the soil with dissolution rates of pristine monomineralic powders determined in the laboratory. This raises two important issues. The extractions were carried out on separated size fractions with the same mass of sample to volume of extractant ratio for each size fraction. This means that for each size fraction the extractions were carried out with different mineral surface area to volume ratios. It is possible that this could have led to the extractant affecting the reactivity of the samples differently. However, this seems unlikely because the trend of reactivity of the size fractions did not follow the trend of surface area to volume of extractant and so it has been assumed that the reactivity of the primary minerals left after the extractions was unaffected by the extractions. The concentration of organic matter and amorphous oxides varied between grain size fractions. Intuitively, the presence of organic matter and amorphous precipitates will have some effect on the way that minerals dissolve in the field[1] thus the results obtained in this study cannot be directly relevant to the field scenario where, for example, the finer grain size fractions may be bound together by precipitates[2] and thus behave as coarse particles. However, the results do mark an important start in comparing the dissolution rates of different size fractions of mineral material in soils to the dissolution rates determined in laboratories on pristine, mono-mineralic powders.

Table 2
Mineralogy (wt.%) of different size fractions as determined by XRD

Size fraction (μm)	Quartz	Plagioclase feldspar	Alkali feldspar	Mica	Chlorite
2000–500	63	16	16	3	2
500–250	62	17	16	3	2
250–53	52	27	12	5	4
53–2	55	24	11	5	5

Subsamples of the 2000–500, 500–250, 250–53 and 53–2 μm fractions were ground to a fine powder; their mineralogy was determined by X-ray diffraction (XRD) following the method of Hooton and Giorgetta (1977) (Table 2) and their major element composition by X-ray fluorescence using a Philips PW1840 XRF spectrometer and the suppliers X40 software (Table 3). Some of the discussion and conclusions reached in this paper rest on the assumption that all the phases present in the mineral size fractions were detected by X-ray diffraction. Detection limits for mineralogical identification in soils using X-ray diffraction are probably in the range of 0–5% and so it is possible that undetected mineral species may be present in the different size fractions at low concentrations. However, the chemistry of the 2000–500 and 500–250 μm fractions and the 250–53 and 53–2 μm fractions are practically identical so it seems reasonable that the mineralogy of these fractions would at least be very similar which, according to the X-ray diffraction analysis, it is. Additionally, modelling of the relative proportions of the different minerals in the samples with a normative computer program, LPNORM (Caritat et al., 1994),

Table 3
Major element chemistry (wt.%) of the different size fractions as determined by XRF

	2000–500 μm	500–250 μm	250–53 μm	53–2 μm
SiO_2	80.1	80.4	70.5	69.5
Al_2O_3	10.1	10.6	16.9	16.3
TiO_2	0.1	0.1	0.5	0.7
Fe_2O_3	0.7	0.7	3.0	3.1
MgO	0.0	0.0	0.3	0.7
MnO	0.0	0.0	0.0	0.1
Na_2O	2.4	2.8	3.3	3.1
CaO	0.3	0.2	0.6	2.1
K_2O	6.3	5.2	4.7	4.3
P_2O_5	0.0	0.0	0.2	0.1

[1] To design laboratory experiments to show this is far from straight forward, for example Hodson (unpublished data) determined far-from-equilibrium dissolution rates of soil mineral fractions before and after the removal of organic material and secondary precipitates. The minerals which had had the organic material and secondary precipitates removed dissolved more rapidly but it is not clear whether this was because the organic material and secondary precipitates inhibited the dissolution of the primary minerals by, for example, blocking reactive sites, or if the organic material and secondary precipitates reacted with the acid in the experiment so that fewer protons were available to react with the primary minerals. If the first scenario is correct, then it is likely that the same thing would happen in the field but if the second scenario is correct, then this is not relevant to the field as organic material and secondary precipitates are likely to be at or close to equilibrium with soil solution. Additionally, some work (Velbel, 1993) has suggested that surface coatings may not affect mineral dissolution rates.

[2] Note in this experiment extractions were carried out on the separated size fractions. Aggregates of fine material would initially have been partitioned into coarser fractions during sieving and then, after removal of precipitates, would have been discarded in the final sieving stage.

using the chemical data in Table 3 gave better fits between the mineralogy and chemistry when only the minerals detected by X-ray diffraction were used as input than when other minerals such as kaolinite were included in the input as minerals present in the soil.

Subsamples of the different grain size fractions were mounted on stubs using double sided sticky tape, carbon coated and analysed in a JEOL JXA840 analytical scanning electron microscope (SEM). Individual grains were analysed to determine their chemical composition using energy dispersive X-ray analysis (EDX). No significant variations between the compositions of the individual mineral species in the different grain size fractions were detected. In addition, analysis of over 300 grains chosen at random failed to identify minerals other than those detected by X-ray diffraction. Average mineral stoichiometries, based in each case on >20 analyses from the 2000–500 μm grain size fraction, were calculated following the method presented in Deer et al. (1966) and are given in Table 4. The analyses of the "mica" grains previously identified by XRD, together with optical microscopy observations indicated that the mica grains were predominantly slightly vermiculised biotite though a small number of muscovite grains were observed. As the muscovite was present in the powders at <1 wt.% levels the "mica" is treated as biotite. Samples were also examined to check that any secondary coatings and organic matter had been removed from the samples and that no fine grained particles were adhered to the surfaces of coarser grains. This proved to be the case (Fig. 1).

Table 4
Average mineral stoichiometry based on >20 electron microscope EDX analyses per mineral species from the 2000–500 μm grain size fraction

	Plagioclase feldspar	Alkali feldspar	Mica	Chlorite
Si	2.89	3.04	6.61	6.75
Al	1.10	0.98	5.26	5.16
Fe[a]	0	0	1.20	4.58
Mg	0	0	0.64	1.63
Na	1.04	0.09	0	0.00
Ca	0.05	0	0	0.00
K	0	0.82	1.65	0.23
O	8	8	24	28

[a] Iron content based on the assumption that all Fe is present as Fe^{3+}.

Finally, uncoated grains from all the size fractions were examined using cathoduluminescence, using a Technosyn Model 8200 Mk II cold stage, to check for the presence of calcite in the samples.

2.2. Dissolution experiments

Batch experiments were carried out on two subsamples of the 2000–500, 500–250, 250–53 and 2–53 μm size fractions, but not the <2 μm fraction for reasons given below. Masses of sample used in the experiments are given in Table 5. Mineral powders were added to 250 ml polypropylene, acid-washed, bottles containing 250 ml of pH 4 HCl. The bottles were placed in a shaking water bath set at 25 °C. Every 7 to 14 days the bottles were removed from the shaker and left to stand for 4 h to give suspended particles time to settle. Because of the problems in determining when <2 μm particles had settled, experiments were not conducted on the <2 μm grain size fraction. Twenty-five millilitres of solution were removed from the bottles using a pipette and filtered through a 0.2-μm filter. Five millilitres of this solution were used for pH measurement. The other 20 ml were acidified to a strength of 2.5% HNO_3 and stored for later analysis. Twenty-five millilitres of fresh, unreacted HCl were then added to each bottle to maintain a constant mass:volume ratio in the experiment before placing it back on the shaker. On the basis of the results (linear increases in element concentration in solution over time), it is assumed that the addition of the 25 ml of fresh solution did not affect significantly the dissolution rates of the mineral powders. A blank experiment, containing no mineral powder but otherwise identical to the other batch experiments, was also run. After c. 14 weeks, the experiments were stopped.

2.3. Solution analysis

All the solutions were analysed by inductively coupled plasma-optical emission spectroscopy (Ca, Si, Al, Fe, Mg) and atomic adsorption spectroscopy (Na, K). Replicate analyses indicate that the precision of these measurements was <2% (2 × standard deviation on six repeat analyses). Quality control was carried out by analysing an in-house standard water solution which had been previously calibrated against a commercially available standard water solution.

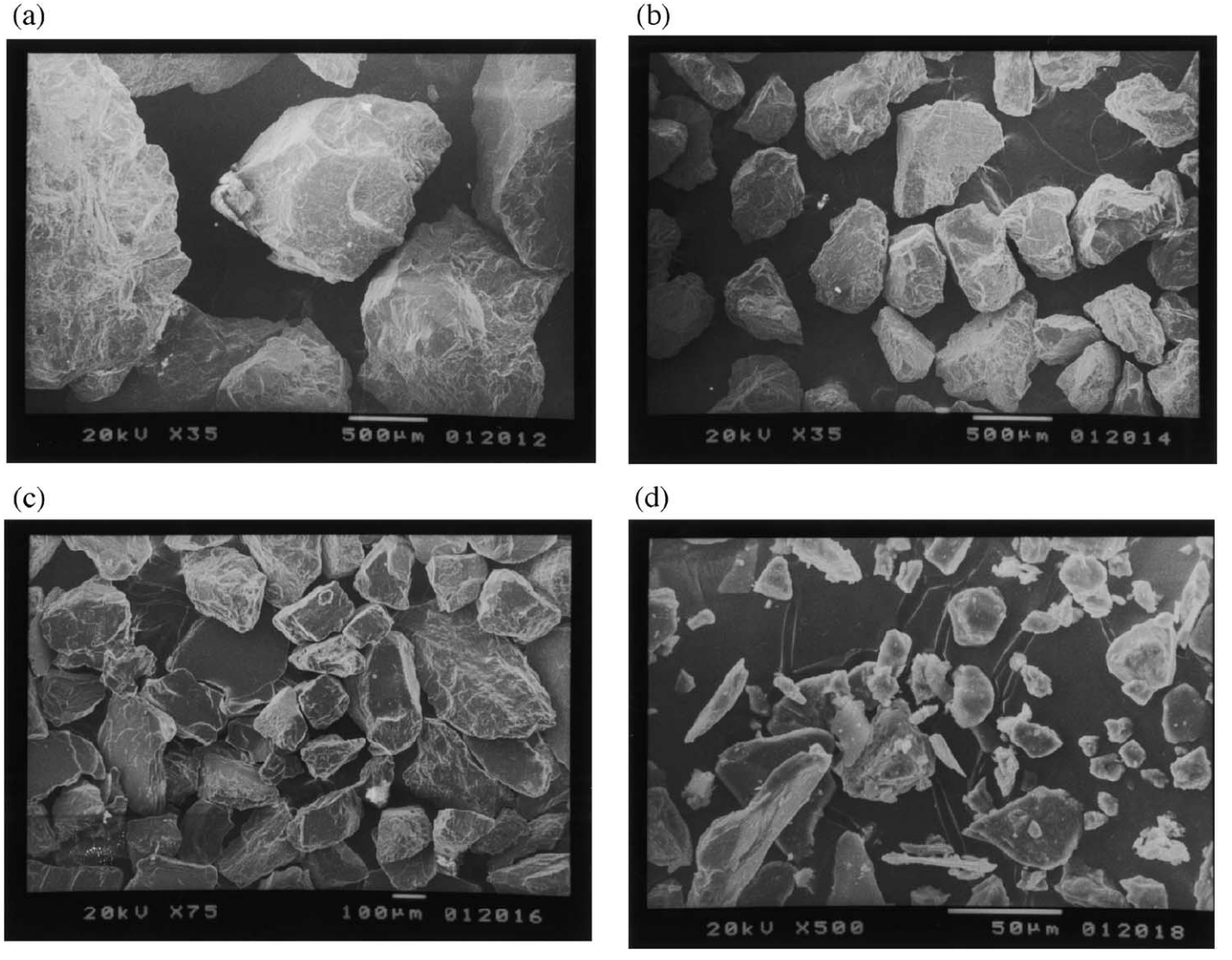

Fig. 1. Secondary electron SEM images of mineral powders prior to dissolution. (a) 2000–500 μm, (b) 500–250 μm, (c) 250–53 μm and (d) 53–2 μm size fractions.

Table 5
Masses of material used in the batch experiments

Size fraction (μm)	Experiment label	Mass of sample used (g)	Total mineral surface area in experiment (m^2)
2000–500	2000–1	2.52	1.08
	2000–2	2.53	1.09
500–250	500–1	2.54	1.75
	500–2	2.72	1.88
250–53	250–1	2.08	3.39
	250–2	2.01	3.28
53–2	53–1	0.56	3.57
	53–2	0.55	3.51
	53–3	0.10	0.66
	53–4	0.12	0.78

Solution compositions were analysed using PHREEQ (Parkhurst and Appelo, 1999) to determine whether they were saturated with any phases. Results of this analysis led to a second set of 53–2 μm experiments being conducted using a smaller mass of sample. These experiments were conducted in an identical fashion to those described above except that, over the course of the first day of the experiment, they were sampled every 1 to 2 h with only 10 min allowed for particle settling before sampling was carried out. This raised the possibility of particles not having time to settle before sampling. However, no particles were observed (by SEM) on the filters through which the solutions from these experiments were filtered, so it has been assumed that the sampling did not remove suspended material from the experiments.

2.4. Element release rate calculations

Surface area normalised element release rates from the mineral powders were calculated in the following fashion.

$$E_{SA} = 0.25m/(60 \times 60 \times A \times M \times SSA) \quad (1)$$

where E_{SA} = rate of element release expressed as moles of element X released per m^2 of solid per second. Note that element release rate is taken to be synonymous with bulk mineral dissolution rate of the powder. Precision of the calculated rates is estimated to be ± 5% on the basis of BET and element concentration determinations. m = the slope of a straight line fitted to a plot of concentration of element X (μg/l) against time

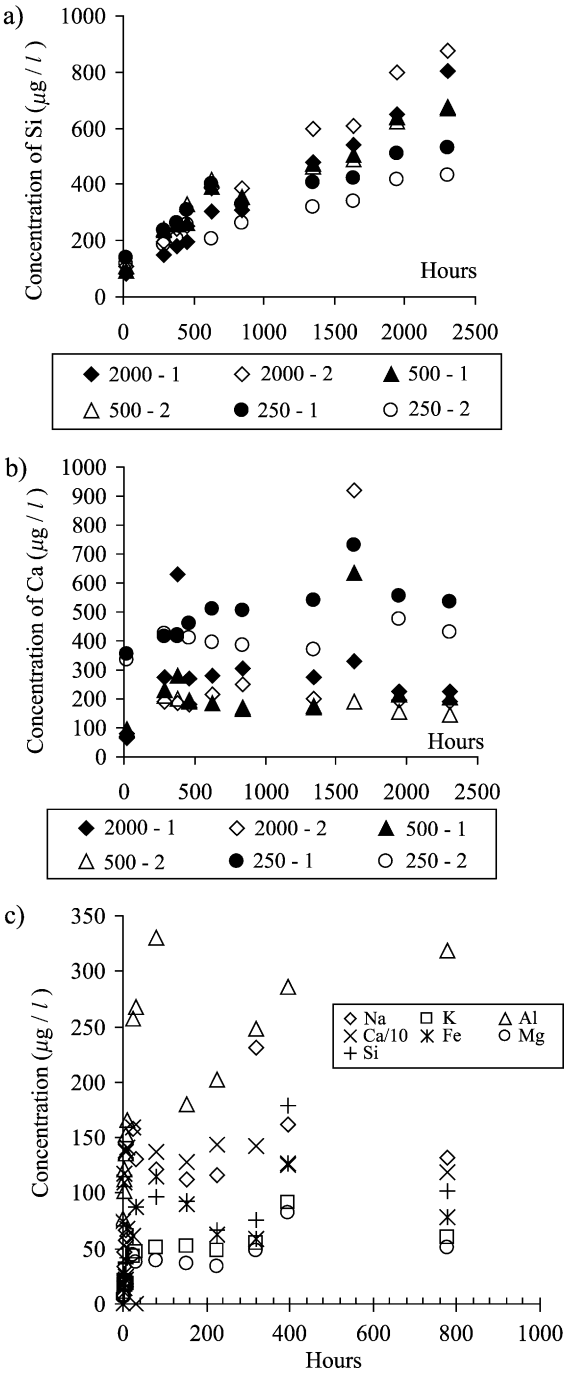

Fig. 2. Changes in (a) Si and (b) Ca concentration with time in the batch experiments (the Ca peak at c. 1500 h is thought to be due to Ca contamination after sampling but prior to analysis), (c) changes in element concentration in experiment 53–3.

(h) for the various experiments (e.g. Fig. 2a). A = atomic mass (μg) of element X, M = mass (g) of mineral grains at the start of the experiment SSA = specific surface area (m^2/g) of the dissolving mineral powder at the start of the experiment.

The 0.25 factor in Eq. (1) is because solution volume in the experiments was 0.25 l.

3. Results

The compositions of the experimental solutions at each sampling interval are given in Appendix A.

3.1. PHREEQ analysis of experimental solutions

Analysis of the experimental solutions using PHREEQ (Parkhurst and Appelo, 1999) indicated that all the solutions were undersaturated with respect to primary and secondary silicates except for the solutions in the initial 53–2 μm experiments (experiments 53–1 and 53–2). These solutions were saturated with respect to kaolinite and K-mica [$KAl_3Si_3O_{10}(OH)_2$] after only 24 h of mineral dissolution. A second set of experiments was therefore conducted on the 53–2 μm fraction (experiments 53–3 and 53–4) using a smaller mass of sample (Table 5) and sampling more regularly than previously. Calculations using PHREEQ indicated that the solutions sampled for these experiments remained undersaturated with respect to primary and secondary silicate phases. Some of the solutions show a slight saturation with respect to haematite (saturation index <0.5) and gibbsite (saturation index <0.2) but, given the low value of these indices, together with the observed linear increases of both Fe and Al concentrations in solution over time, it is not deemed likely that these phases precipitated.

3.2. Changes in solution composition

For the 2000–500, 500–250 and 250–53 μm experiments there was an initial rapid rise in the concentration of elements in solution between the start of the experiment and the first sampling point and then a slower, linear increase in concentration over the duration of the experiment, e.g. Fig. 2a. Such trends are typically observed in monomineralic batch experiments (e.g. Holdren and Speyer, 1985, 1987; Carroll and Walther, 1990; Zhang et al., 1993). Exceptions to the general trend were Ca and Fe which are discussed below. Excepting Ca and Fe, regressions through the concentration data against time, after the removal of any obvious outliers gave RSQ values of ≥ 0.7, except for the K data for experiment 250–2 which had an RSQ value of only 0.5. pH rose initially in all the experiments. In the 2000–500, 500–250 and 250–53 μm experiments it fell back to a relatively constant value greater than the initial pH 4, whereas for 53–3 and 53–4 it remained at its high value.

Iron concentrations in the 2000–500 and 500–250 μm experiments remained below detection levels (3 μg/l) for 620–840 h but then increased in a linear fashion (RSQ = 0.9). In both 250–53 μm experiments, Fe concentrations remained below detection levels until the last sampling event and so release rates of Fe were not calculated for these samples. Iron concentrations in the 53–3 and 53–4 experiments are relatively high and increase linearly over time (RSQ = 0.8 and 0.9) reflecting the higher element release rate in these experiments and the preferential release of Fe relative to the other experiments (see below).

After an initially rapid increase in Ca concentrations in all the experiments, Ca concentrations fluctuated around constant values (Fig. 2b). It was therefore not possible to calculate a Ca release rate based on the changes in solution composition. Reasons for the behaviour of Ca are discussed below.

The changes in solution composition in experiments 53–3 and 53–4 are more puzzling. As in the experiments carried out on the coarser grains there was a rapid initial increase in element concentration between the start of the experiment and the first sampling event followed by a linear increase in concentration (Appendix A). Except for the Ca data from both experiments and the Mg data in experiment 53–4, the RSQ of regressions of concentration against time was ≥ 0.7. However, after 32 h concentrations fluctuated markedly (e.g. Fig. 2c) indicating that the solutions were saturated, though calculations using PHREEQ did not predict this.

3.3. Element release rates

Surface area normalised element release rates are shown in Table 6. The solution composition data used

Table 6
Element release rates normalised to surface area ($10^{14} \times$ mol/m^2/s)

Experiment	Na	Mg	K	Fe	Al	Si
2000–1	13.60	7.46	8.07	2.93	23.23	70.22
2000–2	11.58	7.47	8.25	4.94	23.89	76.69
500–1	8.21	3.33	2.64	0.95	14.61	33.00
500–2	4.18	2.19	1.84	0.62	13.67	28.44
250–1	4.69	1.11	0.93	–	2.46	10.84
250–2	4.93	1.03	0.61	–	5.89	9.76
53–3	3052	451	401	504	2393	758
53–4	1368	296	557	555	2056	440

to calculate the release rates is given in Appendix A. Data from 24–2304 h were used to calculate the 2000–500, 500–250 and 250–53 μm release rates, data for 1–32 h to calculate the 53–2 μm rates.

Several trends stand out in the element release rate data. The element release rates: in the duplicate experiments are generally similar; from the 53–2 μm size fractions are significantly higher than those from the other size fractions, and for the 2000–500, 500–250 and 250–53 μm size fractions decrease with decreasing grain size (RSQ = 0.9–1.0). The release rate of Si compared to the release rate for the other elements is relatively low in the 53–2 μm fraction compared to the other size fractions (Table 7).

The relative contribution of each grain size fraction to element release from the mineral component of the bulk soil (Table 8) was calculated by multiplying the surface area normalised element release rate of the size fraction by the fraction of total mineral surface area provided by that size fraction. For example, the surface area normalised release rate of Na from experiment 2000–1 is 13.60×10^{-14} mol/m^2/s (Table 6) and the surface area fraction of the 2000–500 μm size fraction in the bulk soil is 0.24 (Table 1), thus the calculated contribution of this grain size fraction to Na release from the bulk mineral component of the soil over 1 s is $13.6 \times 10^{-14} \times 0.24 = 3.26 \times 10^{-14}$ mol/$g_{bulk\ soil}$. Relative contributions to element release from the bulk powder decrease in the order 53–2 ≫ 2000–500 > 250–53 ~ 500–250 μm.

Table 7
Surface area normalised element release rates relative to surface area normalised Si release rate for each individual experiment (e.g. Na release rate for 2000–1/Si release rate for 2000–1)

Experiment	Na	Mg	K	Fe	Al	Si
2000–1	0.19	0.11	0.11	0.04	0.33	1
2000–2	0.15	0.10	0.11	0.06	0.31	1
500–1	0.25	0.10	0.08	0.03	0.44	1
500–2	0.15	0.08	0.06	0.02	0.48	1
250–1	0.43	0.10	0.09	–	0.22	1
250–2	0.51	0.11	0.06	–	0.60	1
53–3	4.03	0.59	0.91	0.66	3.16	1
53–4	3.11	0.67	1.27	1.26	4.67	1

Table 8
Number of moles ($\times 10^{14}$) of element released from the different grain fractions as 1 g of bulk soil dissolves for 1 s

Experiment	Na	Mg	K	Fe	Al	Si
2000–1	3.27	1.80	1.94	0.70	5.59	16.91
2000–2	2.79	1.80	1.99	1.12	5.75	18.47
500–1	0.68	0.28	0.22	0.08	1.21	2.73
500–2	0.35	0.18	0.15	0.05	1.13	2.35
250–1	1.53	0.36	0.30	–	0.80	3.54
250–2	1.61	0.33	0.20	–	1.92	3.18
53–3	2142	317	282	354	1679	532
53–4	960	208	391	389	1443	309

Calculated from surface area normalised element release rate × surface area fraction of grain size fraction in bulk soil.

4. Discussion

In terms of answering the question set out at the beginning of this paper, the results clearly show that in this case the finest grain size fraction is the most important in terms of element release from the mineral fractions present in the soil (Table 8). However, the results raise several other interesting points which are discussed below.

4.1. Ca data

It is not clear what the cause of the Ca behaviour was. Lack of Ca in the control experiment indicates that contamination was not the cause. Comparison of the Ca content of the solutions at the end of the experiments with the Ca content of the solid powders shows that, for the 2000–500, 500–250 and 250–53 μm mineral powders, ≤ 1% of the total mass of Ca in the mineral powders was released into solution. For the 53–2 μm powders Ca release into solution comprised 16–18% of the total Ca in the powders. Thus, for all powders Ca remained in the solids at the end of

the experiments so Ca release into solution was not limited by bulk Ca availability.

The PHREEQ calculations indicated that the solutions were undersaturated with respect to Ca-bearing phases so it seems unlikely that Ca concentrations in the solutions were buffered by the precipitation of a Ca-bearing phase. To investigate this further the concentration of Ca in the two 2000–500 μm and the control experiments was increased to c. 1 ppm by addition of $CaCl_2$ solution at the end of the initial experiment. The pH of the solutions was not unduly affected by this procedure. The concentration of Ca remaining in solution was then determined 1 and 7 days after the addition of the $CaCl_2$ solution. Concentrations remained constant indicating that the Ca content was not buffered by the precipitation of a Ca-bearing phase.

Previous studies concerning the dissolution of granite (e.g. White et al., 1999) have shown that (1) many granites contain trace quantities of calcite difficult to detect using XRD of whole rock samples and, (2) preferential dissolution of this calcite accounts for the bulk of Ca release from granites during dissolution. It may be the case that dissolution of small concentrations of calcite in the different grain size fractions resulted in the initial high Ca concentrations in the experimental solutions. Further Ca release due to the dissolution of plagioclase may have been sufficiently slow or have released relatively small quantities of Ca so that the gradual further accumulation of Ca in solution was not detectable. If it is assumed that all the Ca in the experimental solutions was derived from calcite dissolution, the Ca concentrations in the final solutions correspond to dissolution of a mass of calcite $\leq$ 1wt.% of the solid in the experiments. Such concentrations of calcite are hard to detect using conventional techniques. Small (<1 μm) orange spots on feldspar grains were observed when the grains were examined using cathodoluminescence. Whilst calcite does luminesce orange, other minerals may also luminesce orange (Marshall, 1987). Therefore, the presence of calcite in the samples has not been proven and the suggestion that calcite dissolution is controlling Ca release in the experiments must be treated as an unconfirmed hypothesis. An additional problem with this hypothesis is that calcite dissolves in acid ammonium oxalate so, provided that it was only present in small quantities, any calcite may have been removed from the samples during the extraction carried out to remove amorphous precipitates.

4.2. Determining which minerals were dissolving

At the beginning of the experiments it had been planned to apply a modelling code such as NETPATH (Plummer et al., 1994) or carry out a manual calculation after the fashion of Garrels and Mackenzie (1967) in order to determine the relative proportions of the minerals identified in the samples using X-ray diffraction that had dissolved to give the final solution compositions. This proved unfeasible for two reasons.

With the exception of Ca in the plagioclase feldspar, none of the minerals present in the samples contain an element that is not present in significant concentrations in at least one other phase (Table 4). This means that it is not possible to ascribe the concentration of an element in solution to the dissolution of a single unique mineral species. The Ca data could, potentially, be used to determine the number of moles of plagioclase feldspar dissolving. After adjustment for plagioclase dissolution, the Na data could then be used to determine the number of moles of potassium feldspar dissolving. However, as discussed above, it is not clear that the changes in Ca concentration in the experimental solutions are due to the dissolution of plagioclase and so this approach is not valid. Even if it were, it would not be possible to determine the number of moles of mica and chlorite dissolving. This is because the two minerals both contain the same elements so that there is not an element that can be used as a tracer for the dissolution of just one of them.

Calculations of the type carried out by Garrels and MacKenzie (1967) and NETPATH assume stoichiometric or congruent dissolution of minerals. However, examination of the mineral composition data in Table 4, the solution composition data in Appendix A and the element release rates in Table 6 shows that, in many cases in these experiments, the minerals cannot be dissolving congruently. This is illustrated in Fig. 3 where the element release rates of various elements are plotted against each other. For congruent dissolution, element release rates (as moles of element/m^2/s) of different elements should be in the same ratio as the molar ratio of those elements in the minerals which are dissolving. For example, for the congruent dissolution of albite ($NaAlSi_3O_8$), the release rate of Na

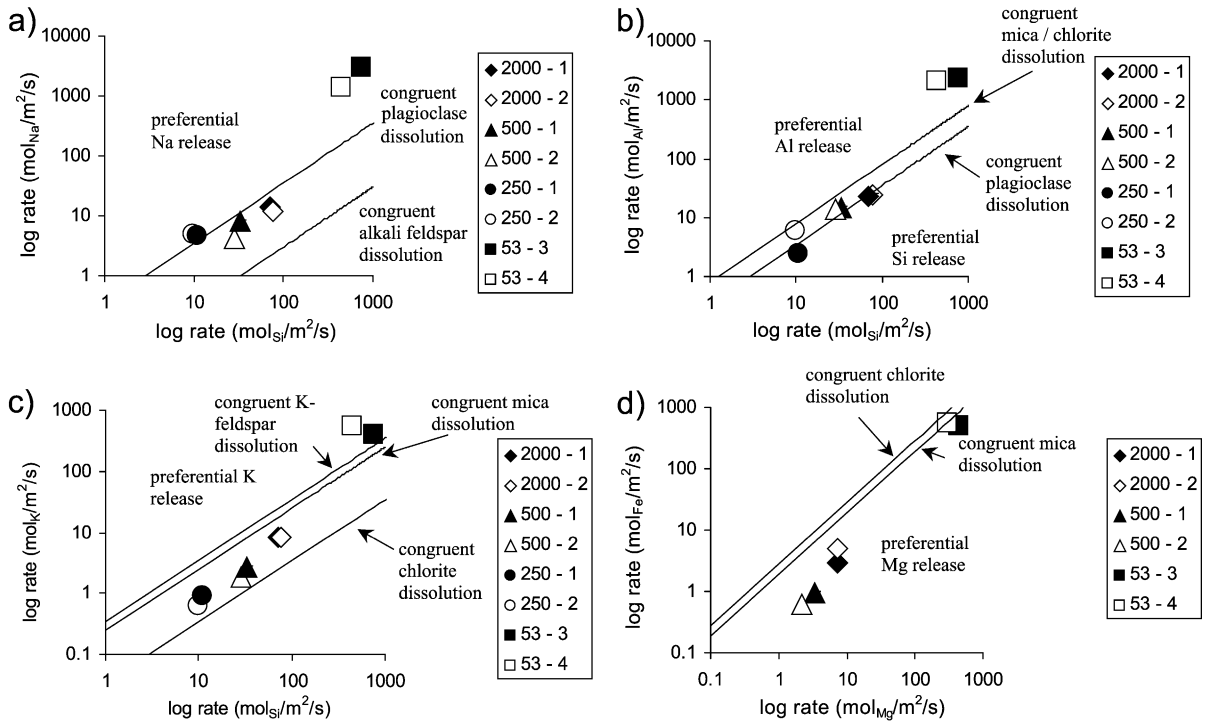

Fig. 3. Plots of element release rate (mol/m^2/s) for the different experiments. (a) Na vs. Si, (b) Al vs. Si, (c) K vs. Si, (d) Fe Vs Mg. Solid diagonal lines show where data resulting from the congruent dissolution rate of specific minerals should plot. Error bars are smaller than symbols.

(mols Na/m^2/s) should be equal to one-third of the release rate of Si (mols Si/m^2/s). Fig. 3a shows that more Na is released from the 53–2 μm fraction than would be expected if the plagioclase and alkali feldspar were dissolving congruently. Fig. 3b and c show that both Al and K release rates are also larger than would be expected for congruent dissolution of the minerals in the 53–2 μm size fraction. Fig. 3a–c indicate that either the minerals in the 53–2 μm fraction are developing cation leached, Si-enriched layers on their surfaces like those observed to form during the initial stages of dissolution in monomineralic laboratory dissolution experiments before steady state dissolution rates have been reached (e.g. Schott et al., 1981; Chou and Wollast, 1984; Oelkers et al., 1994), that silicon precipitation is occurring or that a highly reactive Na–Al–K-rich, Si-poor phase is present in the 53–2 μm size fraction but at too low concentrations to be detected by X-ray diffraction. The first explanation is favoured. Calculations using PHREEQ (Parkhurst and Appelo, 1999) indicate that the solutions from experiments 53–3 and 53–4 are undersaturated with respect to quartz and amorphous SiO_2 and from the soil chemistry and SEM observations there is no reason to suppose that the mineralogy of the 53–2 μm fraction is different from the 250–53 μm fraction. Data for the other size fractions in Fig. 3a–c plot between or on the lines which indicate the ratios of release rates for the congruent dissolution of the different minerals present in the mineral powders. This is consistent with the bulk dissolution rate being the average of dissolution rates due to the congruent dissolution of the different minerals. However, it is possible, though less likely, that the minerals in these size fractions are dissolving incongruently, it being merely serendipitous that the combination of the incongruent dissolution of the phases happens to lie where bulk rates due to congruent dissolution would plot.

In contrast to Fig. 3a–c, the data in Fig. 3d indicate the incongruent dissolution of the sheet silicates in the coarser grain size fractions as the release rate of Mg is

too large with respect to the Fe release rate. It is generally accepted that 2:1 sheet silicates dissolve incongruently (Nagy, 1995). Generally, interlayer ions, typically K^+, are released most rapidly followed by Mg and then Fe from octahedral sheets and then Al and finally Si. The apparent release rate of Fe is slower than that of Mg primarily due to oxidation of Fe^{2+} and reprecipitation as $Fe(OH)_3$. This incongruent behaviour of sheet silicates is seen even under far-from-equilibrium conditions (e.g. Acker and Bricker, 1992). If incongruent dissolution of the sheet silicates in the coarser grain size fractions truly does occur, it is strange (1) that this is not reflected in Fig. 3b and c where release rates of Al and K are plotted against Si release rates respectively and (2) that it does not also occur in the 53–2 μm size fraction given that the mineralogy and chemistry of the 53–2 and 250–53 μm size fractions are practically identical. In addition, analysis of solution compositions using PHREEQ do not indicate that the solutions associated with the coarser grain size fractions are saturated with respect to $Fe(OH)_3$ and although some solutions are slightly saturated with respect to haematite (saturation index <0.5) the linear increases in Fe concentration in solution over time indicate it is unlikely that haematite precipitation is occurring. Interestingly, the Fe and Mg release rate data for the 53–2 μm fraction are consistent with congruent dissolution of the sheet silicates, though from Fig. 3a–c it is clear that this is not happening. Thus, there is evidence for the incongruent dissolution of minerals in all four size fraction experiments and it is therefore not possible to determine which minerals are dissolving in a fashion analogous to the calculations of Garrels and MacKenzie (1967).

The simplest explanation for incongruent dissolution is that the dissolution rate has yet to reach a steady state as is observed in many monomineralic dissolution experiments. This seems unlikely for the coarser grain samples since element concentrations increase linearly over a period of more than 2000 h (Fig. 2a, Appendix A) but may be true for the 53–2 μm fraction. For the coarser fractions the lower than expected Fe release may be due to precipitation of an Fe bearing phase or adsorption of released Fe by the sheet silicates. From the data gathered in this experimental study, it is not possible to choose between these explanations.

4.3. Are the element release rates similar to those determined in laboratory experiments carried out on monomineralic powders?

It is interesting to consider whether the element release rates from the different size fractions are similar to those obtained for dissolution of monomineralic powders in the laboratory. Precise comparisons are, of course, not possible, as the distribution of surface area between the different mineral species in the size fractions is not known. In addition, trace amounts of reactive minerals present at concentrations below the detection limits of X-ray diffraction may be present in the different size fractions giving higher than expected dissolution rates for the bulk sample. The compositions of feldspar present in the mineral powders investigated here approximate to albite and orthoclase. From a compendium of data made by Blum and Stillings (1995; their Figs. 4 and 5), the dissolution rates of albite and orthoclase at 25 °C and c. pH 4 (based on Si release rates) are c. 0.1 and 0.01×10^{-14} mol/m^2/s. These experiments were carried out on grains of diameter 50–250 μm. From data summarised in Nagy (1995) dissolution rates of biotite at 25 °C and c. pH 4 (incongruent dissolution rates based on Si and Mg release rates) are c. 100×10^{-14} mol/m^2/s. Chlorite dissolution rates are similar. These experiments were carried out on grains of diameter c. 150–420 μm, though in some instances the grains were not washed to remove fines.

The rates for monomineralic powders bracket the rates obtained for the 2000–500, 500–250 and 250–53 μm polymineralic powders in the current experiments (Table 6) with the sheet silicate dissolution rates being larger than, and the feldspar dissolution rates being smaller than, the bulk rates reported. This would be expected if the bulk element release rates are some form of average of the dissolution of feldspar, mica and chlorite. However, the dissolution rates for the 53–2 μm powders are generally a factor of 4–30 larger than the monomineralic sheet silicate dissolution rates.

Given that the dissolution rates are surface area normalised, and the distribution of powder surface area between the various mineral species in the size fractions is not known, further comparison of the dissolution rates of the mono- and poly-mineralic powders is not justified. Whilst it is encouraging that

the bulk dissolution rates of the three coarsest fractions are similar to those of the powders' constituent minerals, this does highlight the problem of applying surface area normalised monomineralic dissolution rates to polymineralic powders. The large 53–2 μm element release rates are discussed below but indicate that dissolution rates determined on coarser particles may not be applicable to finer grained material.

4.4. Are similar element release rates expected for the different size fractions?

The next question to be considered is whether the surface area normalised element release rates of the different size fractions would be expected to be the same or not. From Tables 2 and 3 it can be seen that the size fractions split into two chemically and mineralogically distinct groups; both the 2000–500 and 500–250 μm size fractions and the 250–53 and 53–2 μm size fractions are practically identical though this does not preclude the presence of trace amounts of minerals present below the detection limits of X-ray diffraction. The 2000–500 and 500–250 μm size fractions contain more quartz and less plagioclase feldspar than the finer grain size fractions. Given the uncertainties associated with quantitative XRD analysis (Wilson, 1987), the differences in the alkali feldspar (more in the coarser fractions) and sheet silicate (less in the coarser fractions) contents are less certain, though differences in the bulk sample chemistry (Table 3) would seem to support the differences. It might be expected that the 250–53 and 53–2 μm fraction should be more reactive and have higher element release rates than the coarser fractions as plagioclase feldspar (and sheet silicates) is more reactive than quartz (and alkali feldspar) (e.g. Allen and Hajek, 1989; various papers in White and Brantley, 1995).

However, aside from mineralogical differences, differences in relative grain size and shape have to be considered as changes in grain shape can influence the specific surface area of a mineral and thus the surface area available for dissolution and element release. Inspection of Fig. 1 shows that, at least for the 500–250, 250–5 3 and 53–2 μm size fractions, the relative shapes and sizes of the quartz and feldspar grains are the same (grains in the 2000–500 μm fractions were too large to fit several into the SEM field of view). It is hard to measure the dimensions of sheet silicates in the direction perpendicular to their basal cleavage, but for the grains considered here their thickness appears to decrease with decreasing grain size (Fig. 4) though at a lower rate than the other grain dimensions. The implications for element release rates of the bulk powders will be considered for the conditions described above.

Bulk element release rates of mineral powders can be easily calculated using a spreadsheet of the sort shown in Appendix B. Such a spreadsheet was used to investigate the effects of changing mineralogy and grain dimensions on element release rate in the experiments described in this paper. Some results are illustrated in Fig. 5. In this set of calculations, the plagioclase and alkali feldspars were treated as "feldspar" and the biotite and chlorite as "sheet silicate" due to their similar dissolution rates. Dissolution rates were set at 1×10^{-19}, 1×10^{-16} and 1×10^{-12} mol $Si/m^2/s$ for the quartz, feldspar and sheet silicates, respectively, on the basis of literature reported values. Grain dimensions for each size fraction, other than the thickness of the sheet silicates which was varied, were set at the mid-point of the minimum and maximum grain diameters in the size fraction. Surface roughness of grains (the factor by which specific surface area as determined by gas adsorption and the BET isotherm differs from surface area as calculated when regular grain geometries and smooth surfaces are assumed) was initially fixed at a constant value for all mineral types in all grain size fractions. The relative proportions of the different minerals were taken from Table 2.

For these calculations, the bulk element release rate is most sensitive to the surface roughness and dimensions of the sheet silicate and thus its specific surface area and the surface area available for dissolution. This is because the sheet silicate has a dissolution rate 4 orders of magnitude greater than that of the feldspar but is only 1 order of magnitude less abundant.

Fig. 4. Secondary electron images of sheet silicates in the different grain size fractions prior to dissolution. Sheet silicates are oriented with their *z* direction approximately perpendicular to the electron beam allowing thickness to be estimated. (a) 500–250 μm, (b) 250–53 μm and (c) 53–2 μm.

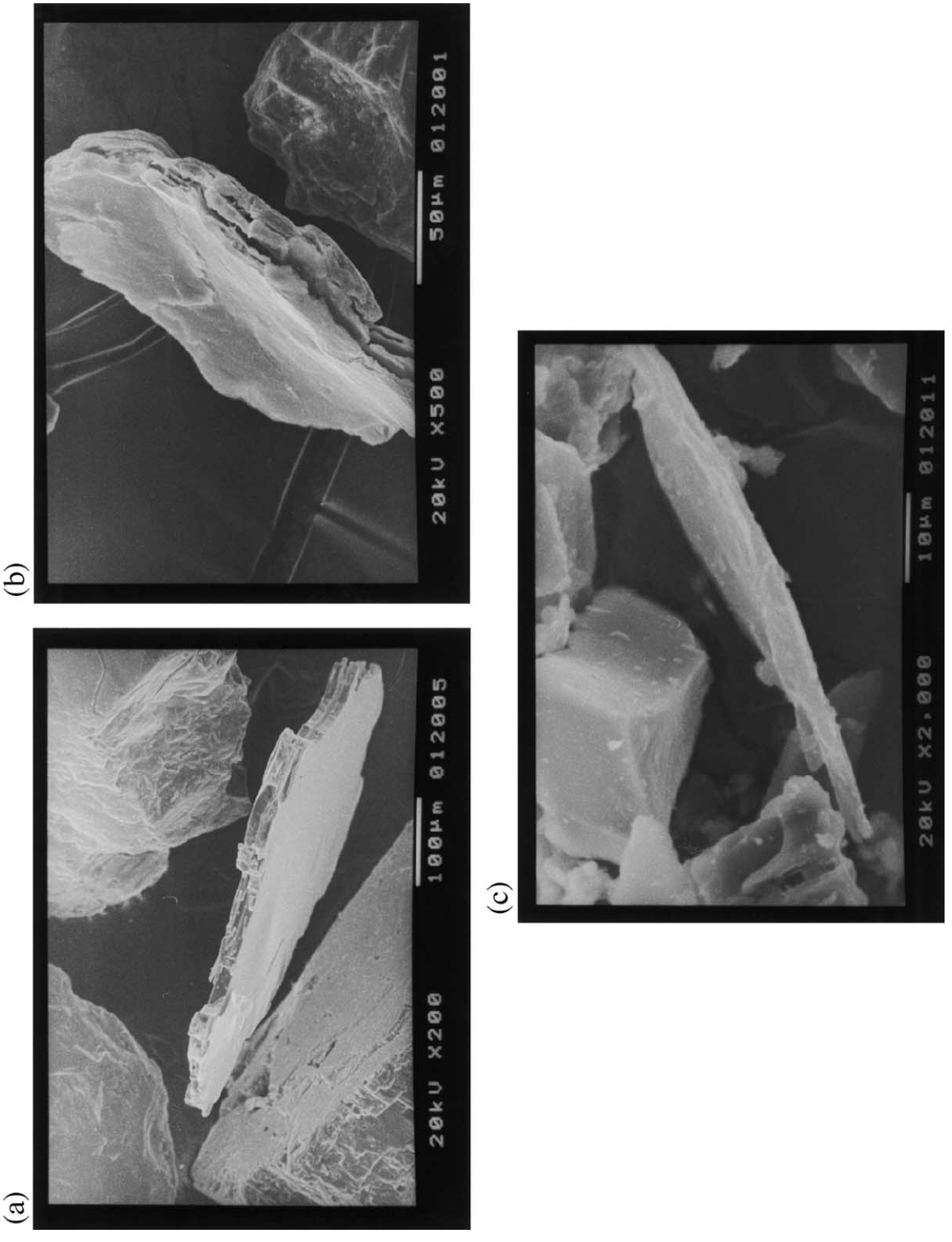
(a)
20kV X200 100µm 012005
(b)
20kV X500 50µm 012001
(c)
20kV X2,000 10µm 012011

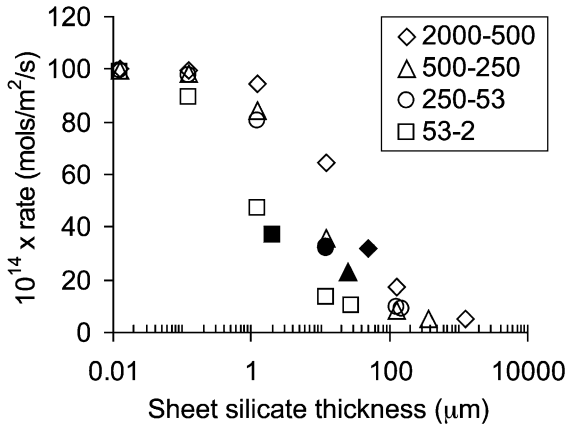

Fig. 5. Variations in calculated bulk element release rate from the different size fractions with varying sheet silicate thickness. The thickest assumed sheet silicate thickness for each size fraction corresponds to cubic sheet silicate grains. Filled symbols are rates calculated for sheet silicate thickness observed by SEM (c. 50, 25, 15 and 2 μm for the 2000–500, 500–250, 250–53 and 53–2 μm fractions).

As shown in Appendix B, for powders of different grain size containing the same minerals in the same proportions and with the same relative dimensions, bulk surface area normalised dissolution rates are constant. For calculations in which the relative dimensions of grains is the same in different size fractions but the proportions of the different minerals present changes, the specific surface area of the individual minerals remains constant but the relative proportion of total surface area occupied by the different minerals changes. Therefore, bulk element release rates vary due to differences in the dissolution rates of the different minerals. In the case of the size fractions considered here, this results in bulk element release rate increasing with decreasing grain size as the finer size fractions contain a higher proportion of sheet silicates (Table 2 and coarsest sheet silicate data points for each size fraction in Fig. 5).

In more realistic calculations, the quartz and feldspar grains were assigned a cubic geometry whilst the sheet silicates were assigned a platy geometry ($x=y>z$). For calculations in which the z dimension of the sheet silicates was kept constant between size fractions, there was a trend of decreasing bulk dissolution rate with decreasing grain size (Fig. 5). As the x and y dimensions of the sheet silicates decreased but the z dimension remained constant, the grains approached a cubic geometry. Although the specific surface area of the grains increased, due to decreasing grain size, the specific surface area of the cubic quartz and feldspar grains, for which all three dimensions reduced, increased more rapidly than that of the platy sheet silicates (e.g. Fig. 6a). Therefore, as grain size decreased in the mixture of cubic and platy grains of constant thickness the fraction of the total surface area of the mixture due to the platy grains decreased (e.g. Fig. 6b). The platy grains, the sheet silicates, had the highest dissolution rate. Therefore, as the proportion of surfaces in the bulk powder due to sheet silicates

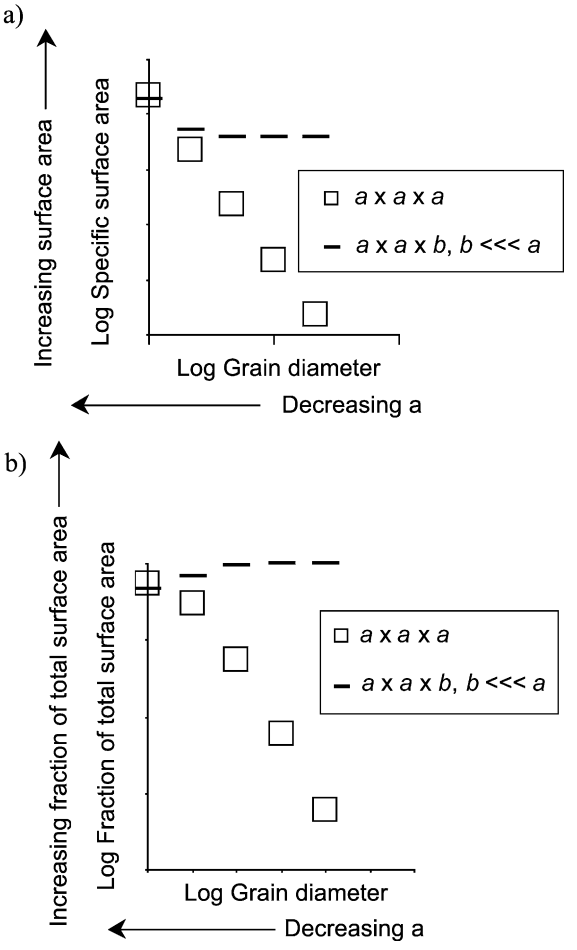

Fig. 6. (a) Changes in specific surface area for grains with dimensions of $a \times a \times a$ and $a \times a \times b$, where $b \ll a$ and b is constant. (b) Changes in contribution to total surface area in a 1:1 by mass mixture of cubes and sheets with decreasing grain size other than constant sheet thickness.

decreased so did the calculated bulk dissolution rate of the powder.

As the sheet silicate thickness decreases, the total surface area of the powders is increasingly dominated by sheet silicate surfaces and so the bulk powder dissolution rates approach that of the sheet silicate and the difference in the dissolution rates of the different size fractions decreases.

For thicknesses of sheet silicates based on SEM observations (thicknesses of c. 50, 25, 15 and 2 μm for the 2000–500, 500–250, 250–53 and 53–2 μm fractions, respectively) (shown as filled symbols in Fig. 5) bulk element release rates from the different size fractions are predicted to be broadly similar (within a factor of 2) and there is no trend in element release rate with grain size. This is due to the effects of changing mineral proportions and the fact that the observed sheet silicate thicknesses do not decrease from one size fraction to the next by the same factor as the mean grain diameters used for the other grain dimensions in the element release rate calculations.

In order to generate significantly larger element release rates in the 53–2 μm fraction than in the other grain size fractions, it was necessary to set the sheet silicate thickness to be far less in the 53–2 μm size fraction than in the other size fractions. Such variations in thickness do not match observations (Fig. 4).

In a second set of calculations, surface roughness of grains was allowed to vary with grain size. Little systematic work has been done on the variation of surface roughness with grain size for weathered grains. White et al. (1996) reported data indicating a decrease in surface roughness with decreasing grain size for the bulk mineral fraction of soils containing quartz, feldspars and hornblende after the removal of secondary minerals. Anbeek et al. (1994) calculated decreasing surface roughnesses with decreasing grain size for weathered feldspars and quartz though the theoretical basis of his calculations is not clear. Neither of these studies deals with sheet silicates but it is possible that surface roughness does decrease with grain size. In this second set of calculations, grain dimensions were set to the mean diameter of each grain size fraction and the observed sheet silicate thickness. Other parameters were kept the same as in the previous set of calculations. Surface roughness was allowed to vary between 1 and 100 for all the grain size fractions. For calculations in which the surface roughness was the same value for all minerals, element release rates are independent of changing surface roughness as the relative surface area of each mineral present in the size fraction remained constant. If the surface roughness of the quartz and feldspar is fixed but the surface roughness of the sheet silicate increases, the calculated element release rate from a given size fraction increases (e.g. Fig. 7) as a higher proportion of the total surface area of the size fraction is due to the more rapidly dissolving sheet silicates. However, in order to generate a trend of decreasing element release rate with decreasing grain size, using the observed sheet silicate thicknesses, it is necessary to set the surface roughness of the sheet silicates in the 2000–500 and 500–250 μm size fractions to be 4–5 orders of magnitude greater than that of the quartz and feldspar whilst the surface roughnesses of the sheet silicates in the two finer fractions have to be similar to the values for the quartz and feldspar and at least 3 orders of magnitude less than those for the sheet silicates in the coarser fractions. This would seem to be unrealistic and certainly involves a greater variation in surface roughness with grain size than reported by White et al. (1996) or Anbeek et al. (1994).

To generate significantly larger dissolution rates in the 53–2 μm fraction compared to the other size fractions requires the surface roughness of the sheet

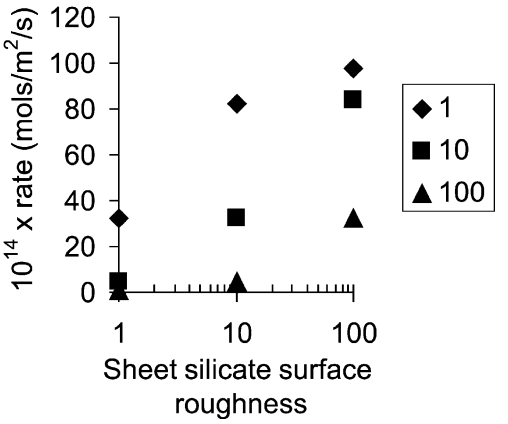

Fig. 7. Changes in the bulk element release rates calculated for the 2000–500 μm size fraction using the same parameters as in Fig. 5 but varying values for surface roughness of the sheet silicate (*x* axis) for surface roughnesses for quartz and feldspar of 1 (diamonds), 10 (squares) and 100 (triangles).

silicates in the 53–2 μm fraction to be significantly (several orders of magnitude) larger than the surface roughness in the other size fractions whilst the surface roughnesses of the feldspar and quartz are several orders of magnitude lower than those in the coarser fractions. This would appear to be unrealistic when considered in the light of the variation in surface roughness and grain size reported by White et al. (1996) or Anbeek et al. (1994).

4.5. Comparing the predicted and actual bulk dissolution rate trends

The distinct trend of decreasing element release rate with decreasing grain size seen for the three coarsest fractions has a high statistical significance (RSQ = 0.9–1.0) and is thought to be real. However, using a geometrical model of the type in Appendix B, such a trend is only realistically reproduced if sheet silicates thickness is kept constant and greater than c. 0.1 μm (Fig. 5). Although the SEM observations indicate that sheet silicate thickness does not remain constant with decreasing grain size (Fig. 4), this treats the sheet silicates as solid blocks of mineral. As can be seen in Fig. 4, the sheet silicates have begun to exfoliate, with the blocks of sheet silicate splitting into thinner blocks. It was not possible to determine the average thickness of blocks that the sheet silicates in the different size fractions were splitting into but depending on the controls on exfoliation (for example it may be a self-organising system with "preferred", stable split block thicknesses existing) the sheet silicates may be closer to having a constant thickness than previously suggested. In which case the observed decrease in dissolution rate with grain size would match theoretical predictions.

It did not prove possible to predict the significantly larger dissolution rate of the 53–2 μm fraction without making unrealistic assumptions regarding sheet silicate thickness or surface roughness. It is therefore not clear why the dissolution rate of the 53–2 μm fraction should be so large and the first question to be considered is whether the concentration data for the 53–2 μm experiments represent the initial rapid rise in element concentration in solution observed in the other experiments or a steady state dissolution rate. Although the linear increase in element concentration favours an interpretation of the data as representing steady state dissolution, the lack of congruent dissolution in the 53–2 μm experiments (Fig. 3a–c) indicate that dissolution has not yet reached a steady state (see above).

To resolve this issue required the 53–2 μm experiments to be run for a longer period of time. However, as is seen in Fig. 2c, after 32 h of dissolution, solution compositions began to fluctuate. Although calculations using PHREEQ do not predict saturation of the solutions (other than the slight saturation with respect to haematite), this is the most obvious explanation for the fluctuations since they were not seen in the control experiment. Although this interpretation is problematic given that apart from the relatively high Fe concentrations, concentrations are similar to the other, undersaturated, experiments, the effect is seen in both duplicate experiments and not the control and is therefore not thought to be an experimental artefact. Because of the fluctuations, it was not possible to calculate an element release rate for the 53–3 and 53–4 experiments over a longer period of dissolution. Thus, it is not certain whether the dissolution rates calculated from the 53–3 and 53–4 data represent initial, rapid, or later, slower dissolution rates. However, some useful points can still be raised.

With the exception of Si, the concentration of elements in solutions from experiments 53–3 and 53–4 after 24 h of dissolution is greater than the concentration of elements in solution after 24 h of dissolution of the other powders (Appendix A) despite the 53–3 and 53–4 experiments containing less surface area (Table 5). Concentrations of elements in solution after 24 h normalised to surface area (data not plotted) again show that, apart from for Si, element release is more rapid from the 53–2 μm fraction than from the other size fractions. The reason for the relatively slow Si release from the 52–2 μm fraction compared to the other elements released from this fraction may be due to precipitation of a Si bearing phase (through PHREEQ predicts that the solutions are undersaturated with respect to such phases), or (more likely) the development of Si-depleted layers on the grain surfaces. The initial 53–1 and 53–2 experiments also indicated more rapid dissolution of this fraction. The experimental solutions were saturated with respect to kaolinite and mica after just 24 h of dissolution, yet the solutions from the 250–53 μm experiments were

not despite experiments 250–1 and 250–2 containing the same minerals in essentially the same proportions and having the same amount of mineral surface present (Tables 2 and 5) (again this assumes that the 53–2 μm does not contain a highly reactive phase at concentrations below the detection limit of X-ray diffraction). This indicates that the 53–2 μm powders dissolve more rapidly than the others. Thus, it would appear that whilst the larger element release rates calculated for the 53–2 μm fractions may not be steady state values, the 53–2 μm fraction does dissolve more rapidly than the other size fractions. Drever (1994) suggested that one of the mechanisms by which land plants could influence weathering rates of silicate minerals is by binding fine particles in the soil. Certainly, the results presented here indicate that retaining fine grained particles in the soil would greatly increase the weathering rate of the soil.

Finer grains may be more soluble than coarser ones due to surface free energy effects (Nielsen, 1964; Holdren and Berner, 1979). Holdren and Berner (1979) show an equation, taken from Schindler et al. (1965), relating surface free energy and grain size to solubility product:

$$\ln\left[\frac{K_{\text{spgrain}}}{K_{\text{spbulk}}}\right]\frac{2\sigma bM}{3\rho RT}\left(\frac{1}{r}\right) \quad (2)$$

where K_{spgrain} = solubility product of the grain in question, K_{spbulk} = solubility product of the bulk solid, σ = specific surface free energy (erg cm^{-2}), b = geometric factor = 3 for spheres and 6 for cubes, M = molecular weight (g mol^{-1}), ρ = density (g cm^{-3}), R = gas constant = 8.3147×10^7 erg mol^{-1} deg^{-1}, T = absolute temperature (K), r = radius of grain in question (cm).

The problem with applying equations such as the one above lie in the uncertainty associated with the specific surface free energy term. Holdren and Berner (1979) estimate that, as a first approximation, and taking into account the hardness of albite, its low solubility and the work of Langmuir (1971), Schindler et al. (1965) and Nielsen and Söhnel (1971), the specific free energy of albite is 600 erg cm^{-2}. This value has been adopted as a general value for all the silicates in the samples dissolved in the current experiments Using this value in Eq. (2) shows that the solubility product of grains with an average diameter of 27.5 μm (the mid-point of the 53–2 μm size fraction) would be about half an order of magnitude greater than the solubility product of grains with an average diameter of 150 μm (the mid-point of the 250–53 μm size fraction). Holdren and Speyer (1985, 1987) use the fact of higher solubility products to explain the more rapid dissolution of small (< 1 μm) grains. If extended to coarser, 53–2 μm grains, this hypothesis would fit the data presented here. Clearly, a large amount of uncertainty is associated with this calculation due to the estimated surface free energy term. In addition, caution should be exercised in relating solubility to dissolution rates. For example, Valsami-Jones et al. (1998) found that synthetic apatite, though 12 orders of magnitude more soluble than natural apatite, dissolved 2 orders of magnitude more slowly though this difference may have been due to the different nature of the two materials, one was synthetic, the other natural. However, in the current experiments, particularly the 250–53 and 53–2 μm experiments, the material is practically identical other than grain size differences so it seems more reasonable to expect a more soluble finer fraction to dissolve more rapidly.

An alternative explanation for the large element release rates from the 53–2 μm fractions is that the BET surface area which was used to normalise mineral dissolution rates is not proportional to the reactive surface area of the grains. This issue has been raised in the past with regard to alkali feldspars (e.g. Lee and Parsons, 1995; Lee et al., 1998). In this case, the 53–2 μm fractions would have a far larger reactive surface area than the other size fractions. However, why this might be the case is not clear. For example, etch pits on feldspars are thought to represent sites where preferential dissolution has occurred. Scanning electron microscope examination of individual grains indicates that feldspars from all size fractions may be equally pitted and were thus equally reactive whilst dissolving in the soil. In addition, experiments have shown that whilst in nature the distribution of reactive sites on mineral grains does effect dissolution rates, in laboratory experiments where dissolution occurs far from equilibrium, the effect is negligible (Lee et al., 1998).

The calculations based on Appendix B and illustrated in Figs. 5 and 7 ignore surface energy effects and assume that all exposed surface area is equally

reactive. Therefore, if either of the above hypotheses is correct, they could explain the unpredicted large element release rate from the 53–2 μm size fraction. In addition, the experimentally determined rates to which the rates determined in these experiments were compared were generally determined on coarser grain size fractions than 53–2 μm. If either of the above two hypotheses is correct, then for the dissolution rate of fine grained material to be predicted from laboratory determined dissolution rates will require laboratory experiments to be conducted on fine grained material.

Further discussion of the differences in the dissolution rate are beyond the scope of this paper but the current results point the way forward to important lines of research in the future.

5. Conclusions

The main finding in this study was that the finest grained size fraction investigated was the most important for element release. The reason for the large dissolution rate of this fraction is not clear but (provided that the mineralogical analysis has not failed to identify low concentrations of highly reactive minerals in this fraction which are absent in the other fractions, and that the chemical extractions did not effect the reactivity of the different size fractions differently—both these caveats seem unlikely and are discussed above) it implies that either: (1) the reactivity of particles in the finest grain size fraction is greater than the reactivity of the grains in the coarser fractions and/or (2) the finer size fraction has a greater reactive surface area than the other fractions which is not proportional to BET surface area. If this trend continued, the <2 μm grain size fraction would be more important still for element release.

It was shown that the element release rates of the three coarser bulk mineral powders fell between the dissolution rates determined for monomineralic powders of the constituent minerals of the bulk powders. However, these rates cannot be compared to any great extent due to a lack of knowledge of the distribution of surface area between different minerals in the mineral powders. In addition, the element release rate of the 53–2 μm fractions was significantly greater than the laboratory determined dissolution rates of sheet silicates raising the prospect that the laboratory rates are not applicable to fine grained material.

Similar experiments to those described now need to be carried out on a range of soils to see if the same results are obtained. These experiments are currently being repeated using a flow through reactor. If laboratory experiments carried out on pristine mineral grains with no coatings or organic material or secondary precipitates provide meaningful information regarding the rates and mechanisms by which minerals dissolve in soils, and if the current results are more universally applicable, it implies that any dissolution experiments carried out on monomineralic powders with the express purpose of generating data to try and allow the prediction of mineral weathering rates in the field should be carried out using fine grained material. If experiments are carried out on coarse material, the increase in reactivity with decreasing grain size due to surface energy effects must be taken into account when extrapolating rates to the field.

Acknowledgements

Mike Andrews (XRD, PRIS, Reading University), Anne Dudley (ICP-OES, AAS, Department of Soil Science, Reading University), Terry Greenwood (SEM, Natural History Museum, London), Anne Johnstone (soil sampling, Department of Geology and Geophysics, Edinburgh University), Justine Ponzzi (SEM, PRIS, Reading University), Franz Street (XRF, PRIS, Reading University) and Dave Thornley (BET, PRIS, Reading University) are thanked for technical assistance. An anonymous reviewer and Susan Brantley are thanked for their reviews of the manuscript. The author gratefully acknowledges the hospitality of the Natural History Museum in London where he is a Scientific Associate and was able to write this paper in relative peace and quiet. **[EO]**

Appendix A

Concentration data (μg/l) for experiments 2000–1, 2000–2, 500–1, 500–2, 250–1, 250–2, 53–3 and 53–4 used to calculate dissolution rates. $<$DL = below detection limits; these were of the order 5 μg/l (Na), 0.1 μg/l (Mg), 0.2 μg/l (K), 3 μg/l (Fe), 6 μg/l

(Al) and 2 μg/l (Si) and were set to = mean + 6 × standard deviation on six analyses of a reagent blank. r^2 refers to the RSQ for a regression of concentration against time. Figure in italics were not included in the regression as they appear to be erroneous.

Hours	Na	Mg	K	Fe	Al	Si	pH
2000–1							
24	50	6	19	<DL	*37*	81	4.1
288	90	28	27	<DL	0	149	4.4
384	91	31	39	<DL	0	182	4.2
456	81	29	37	*49*	0	197	4.9
624	96	36	52	<DL	25	302	5.4
840	127	51	32	22	62	309	4.4
1344	130	58	46	37	105	482	4.6
1632	142	61	53	35	130	543	4.9
1944	159	72	126	41	164	648	4.3
2304	168	77	144	45	212	802	4.4
r^2	0.9	0.9	0.8	0.9	0.9	1.0	0.2
2000–2							
24	43	7	14	*42*	59	110	3.6
288	48	24	46	<DL	15	196	4.9
384	46	26	48	<DL	31	241	5.0
456	58	28	58	<DL	43	250	4.9
624	92	39	*71*	<DL	67	385	4.7
840	*132*	48	38	38	108	386	4.4
1344	119	57	54	56	143	596	4.4
1632	*132*	*115*	61	54	164	608	4.6
1944	119	72	142	69	205	798	4.0
2304	125	74	150	69	242	877	4.4
r^2	0.9	0.9	0.7	0.9	0.9	1.0	0.0
500–1							
24	21	6	<DL	<DL	33	93	4.1
288	36	*415*	26	<DL	<DL	238	4.9
384	24	23	21	<DL	27	260	4.9
456	27	22	29	<DL	41	262	4.7
624	28	25	31	<DL	58	392	5.0
840	53	30	16	11	99	255	4.5
1344	61	38	25	17	133	474	4.4
1632	88	*79*	26	15	156	506	4.5
1944	86	52	70	24	193	639	4.3
2304	134	56	78	23	220	677	4.5
r^2	0.9	1.0	0.7	0.9	1.0	1.0	0.1
500–2							
24	42	7	4	<DL	31	108	4.0
288	21	26	21	<DL	16	240	4.7
384	20	24	20	<DL	29	260	4.8
456	26	24	23	<DL	40	329	4.6
624	35	27	28	<DL	60	417	5.0
840	52	31	12	10	95	357	4.5
1344	63	39	22	13	128	464	4.3

Appendix A (*continued*)

Hours	Na	Mg	K	Fe	Al	Si	pH
1632	69	39	24	16	255	491	4.4
1944	69	45	53	16	289	622	4.4
2304	77	45	60	16	232	668	4.5
r^2	0.8	0.9	0.7	0.9	1.0	0.9	0.0
250–1							
24	27	13	<DL	<DL	*153*	139	4.0
288	25	20	8	<DL	<DL	240	5.3
384	31	20	5	<DL	<DL	264	5.1
456	40	21	15	<DL	<DL	307	5.0
624	51	26	14	<DL	<DL	402	5.5
840	69	28	8	<DL	<DL	331	5.0
1344	88	34	11	<DL	17	408	4.7
1632	112	50	16	<DL	22	424	4.8
1944	117	43	38	<DL	41	513	4.6
2304	127	43	44	4	72	532	4.7
r^2	1.0	1.0	0.8	0.4	0.9	0.9	0.0
250–2							
24	14	12	8	<DL	*124*	117	3.8
288	15	18	13	<DL	<DL	185	5.3
384	11	17	<DL	<DL	<DL	204	5.1
456	20	17	12	<DL	<DL	257	5.0
624	20	16	7	<DL	20	207	5.4
840	36	17	6	<DL	45	261	4.8
1344	44	18	10	<DL	65	317	4.5
1632	70	*106*	10	<DL	89	342	4.6
1944	135	45	40	<DL	116	417	4.5
2304	105	35	29	3	143	432	4.5
r^2	0.8	0.7	0.5	0.4	1.0	0.9	0.1
53–3							
1.1	<DL	6	<DL	<DL	77	58	4.2
2.2	<DL	7	<DL	10	101	27	4.2
3.0	47	8	17	14	113	27	4.2
4.0	34	6	11	18	121	27	4.2
5.4	58	18	21	22	136	36	4.3
7.4	67	21	17	25	153	38	4.3
9.4	62	20	18	68	166	41	4.2
24.2	158	44	43	61	257	113	4.2
32.0	131	38	47	88	267	87	4.3
r^2	0.8	0.9	0.9	0.8	0.9	0.7	0.1
53–4							
1.1	<DL	6	<DL	<DL	82	37	4.2
2.2	18	7	15	11	110	30	4.3
3.0	15	7	11	19	130	31	4.3
4.0	21	7	14	22	135	30	4.3
5.4	17	7	<DL	24	158	38	4.5
7.4	67	28	21	*539*	196	*95*	4.3
9.4	69	21	25	34	178	41	4.3
24.2	78	24	27	61	266	62	4.3
32.0	119	22	99	123	288	67	4.3
r^2	0.8	0.5	0.7	0.9	0.7	0.9	0.1

Appendix B

Schematic spreadsheet for determining the surface area normalised dissolution rate of a mineral powder comprising several different minerals.

Consider a mixture of three minerals A, B and C.

	Mineral A	Mineral B	Mineral C
Fixed parameters			
Density ρ (kg/m^3)	ρ_a	ρ_b	ρ_c
x dimension (m)	a_x	b_x	c_x
y dimension (m)	a_y	b_y	c_y
z dimension (m)	a_z	b_z	c_z
Mass of mineral/mass of mixture, f	f_a	f_b	f_c
Dissolution rate (mol/m^2/s), d	d_a	d_b	d_c
Surface roughness,* λ	λ_a	λ_b	λ_c
Calculations			
Volume (m^3) = xyz	V_a	V_b	V_c
Surface area (m^2) = $\lambda \times (2xy + 2yz + 2zx)$	SA_a	SA_b	SA_c
Specific surface area (m^2/g) = SSA = $\lambda \times (2xy + 2yz + 2zx)/(\rho \times xyz)$	SSA_a	SSA_b	SSA_c
Dissolution rate of mineral in Mg of soil (mols/s) = $M \times f \times$ SSA $\times d$	R_a	R_b	R_c
Total dissolution rate (mol/s) = $R_a + R_b + R_c = R_{bulk}$			
Total surface area normalised dissolution rate (mol/m^2/s) = $R_{bulk}/M[(f_a \times SSA_a)+(f_b \times SSA_b)+(f_c \times SSA_c)]$			

If we then consider the same distribution of minerals, with the same relative sizes and shapes, but a factor of P smaller

	Mineral A	Mineral B	Mineral C
Fixed parameter			
Density $\rho_{a,b,c}$ (kg/m^3)	ρ_a	ρ_b	ρ_c
x dimension (m)	a_x/P	b_x/P	c_x/P
y dimension (m)	a_y/P	b_y/P	c_y/P
z dimension (m)	a_z/P	b_z/P	c_z/P
Mass of mineral/mass of mixture, $f_{a,b,c}$	f_a	f_b	f_c
Dissolution rate (mol/m^2/s), d	d_a	d_b	d_c
Surface roughness, λ	λ_a	λ_b	λ_c
Calculations			
Volume (m^3) = xyz	V_a/P^3	V_b/P^3	V_c/P^3
Surface area (m^2) = $\lambda \times (2xy + 2yz + 2zx)$	SA_a/P^2	SA_b/P^2	SA_c/P^2
Specific surface area (m^2/g) = SSA = $\lambda \times (2xy + 2yz + 2zx)/(\rho \times xyz)$	$P \times SSA_a$	$P \times SSA_b$	$P \times SSA_c$
Dissolution rate of mineral in Mg of soil (mol/s) = $M \times f \times$ SSA $\times d$	$P \times R_a$	$P \times R_b$	$P \times R_c$
Total dissolution rate (mol/s)=$(P \times R_a)+(P \times R_b)+(P \times R_c) = P \times R_{bulk}$			
Total surface area normalised dissolution rate (mols/m^2/s) = $P \times R_{bulk}/M(f_a \times P \times SSA_a)+(f_b \times P \times SSA_b)+(f_c \times P \times SSA_c)]$ = $R_{bulk}/M(f_a \times SSA_a)+(f_b \times SSA_b)+(f_c \times SSA_c)]$ i.e. the same as for the coarser grain size fraction			

* The factor by which specific surface area differs from geometric surface area.

References

Acker, J.G., Bricker, O.P., 1992. The influence of pH on biotite dissolution and alteration kinetics at low temperature. Geochim. Cosmochim. Acta 56, 3073–3092.

Allen, B.I., Hajek, B.F., 1989. Mineral occurrence in soil environments. In: Dixon, J.B., Weed, S.B. (Eds.), Minerals in Soil Environments. Soil Sci. Soc. Am., Madison, WI, USA, pp. 199–278.

Anbeek, C., van Breemen, N., Meijer, E.L., van der Plas, L., 1994. The dissolution of naturally weathered feldspars and quartz. Geochim. Cosmochim. Acta 58, 4601–4610.

Bain, D.C., Mellor, A., Wilson, M.J., Duthie, D.M.L., 1994. Chemical and mineralogical weathering rates and processes in an upland granitic till catchment in Scotland. Water Air Soil Pollut. 73, 11–27.

Berner, R.A., 1995. Chemical weathering and its affect on atmospheric CO_2 and climate. In: White, A.F., Brantley, S.L. (Eds.), Chemical Weathering Rates of Silicate Minerals. Reviews in Mineralogy, vol. 31. American Mineralogical Society, Washington, USA, pp. 565–583.

Blum, A.E., Stillings, L.L., 1995. Feldspar dissolution kinetics. In: White, A.F., Brantley, S.L. (Eds.), Chemical Weathering Rates of Silicate Minerals. Reviews in Mineralogy, vol. 31. American Mineralogical Society, Washington, USA, pp. 291–351.

Bock, R., 1979. A handbook of decomposition methods in analytical chemistry. International Textbook Company, Glasgow, Scotland, p. 444.

Brunauer, S., Emmett, P.H., Teller, E., 1938. Adsorption of gases in multimolecular layers. J. Am. Chem. Soc. 60, 309–319.

Caritat, P., de Bloch, J., Hutcheon, I., 1994. LPNORM: a linear programming normative analysis code. Comput. Geosci. 20, 313–347.

Carroll, S.A., Walther, J.V., 1990. Kaolinite dissolution at 25°, 60° and 80 °C. Am. J. Sci. 290, 797–810.

Chou, L., Wollast, R., 1984. Study of the weathering of albite at room temperature and pressure with a fluidized bed reactor. Geochim. Cosmochim. Acta 48, 2205–2218.

Deer, W.A., Howie, R.A., Zussman, J., 1966. An Introduction to the Rock-forming Minerals. Longman, Harlow, UK, p. 528.

Drever, J.I., 1994. The effect of land plants on weathering rates of silicate minerals. Geochim. Cosmochim. Acta 58, 2325–2332.

Garrels, R.M., Mackenzie, F.T., 1967. Origin of the chemical compositions of some springs and Lakes. Equilibrium Concepts in Natural Water Systems: Advances in Chemistry Series no. 67. American Chemical Society, Washington, DC, USA, pp. 222–242.

Holdren, G.R., Berner, R.A., 1979. Mechanism of feldspar weathering—I. Experimental studies. Geochim. Cosmochim. Acta 43, 1161–1171.

Holdren, G.R., Speyer, P.M., 1985. Reaction rate–surface area relationships during the early stages of weathering—I. Initial observations. Geochim. Cosmochim. Acta 49, 675–681.

Holdren, G.R., Speyer, P.M., 1987. Reaction rate–surface area relationships during the early stages of weathering—II. Data on eight additional feldspars. Geochim. Cosmochim. Acta 51, 2311–2318.

Hooton, D.H., Giorgetta, N.E., 1977. Quantitative X-ray diffraction analysis by direct calculation method. X-ray Spectrom. 6, 2–5.

Hornung, M., Bull, K.R., Cresser, M., Hall, J., Langan, S.J., Loveland, P., Smith, C., 1995. An empirical map of critical loads of acidity for soils in Great Britain. Environ. Pollut. 90, 301–310.

Langmuir, D., 1971. Particle size effect from the reaction: goethite = hematite + water. Am. J. Sci. 271, 147–156.

Lee, M.R., Parsons, I., 1995. Microtextural controls on weathering of perthitic alkali feldspars. Geochim. Cosmochim. Acta 59, 4465–4488.

Lee, M.R., Hodson, M.E., Parsons, I., 1998. The role of intragranular microtextures and microstructures in chemical and mechanical weathering: direct comparisons of experimentally and naturally weathering alkali feldspar. Geochim. Cosmochim. Acta 62, 2771–2788.

Marschner, H., 1995. Mineral Nutrition of Higher Plants. Academic Press, New York, USA, p. 889.

Marshall, D.J., 1987. Cathodoluminescence of Geological Materials. Unwin Hyman, London, UK, p. 146.

McKeague, J.A., Day, J.H., 1966. Dithionite- and oxalate-extractable Fe and Al as aids in differentiating various classes of soils. Can. J. Soil Sci. 46, 13–22.

Nagy, K.L., 1995. Dissolution and precipitation kinetics of sheet silicates. In: White, A.F., Brantley, S.L. (Eds.), Chemical weathering rates of silicate minerals. Reviews in Mineralogy, vol. 31. American Mineralogical Society, Washington, USA, pp. 173–233.

Nielsen, A.E., 1964. Kinetics of Precipitation. Macmillan, Oxford, UK.

Nielsen, A.E., Söhnel, O., 1971. Interfacial tensions electrolyte crystal-aqueous solution from nucleation data. J. Cryst. Growth 11, 233–242.

Oelkers, E.H., Schott, J., Devidal, J.L., 1994. The effect of aluminium, pH and chemical affinity on the rates of aluminosilicate dissolution reactions. Geochim. Cosmochim. Acta 58, 2011–2024.

Parkhurst, D.L., Appelo, C.A.J., 1999. User's guide to PHREEQ (version 2). Water Resources Investigations Report 99-4259. United States Geological Survey.

Plummer, N.L., Prestemon, E.C., Parkhurst, D.L., 1994. An interactive code (NETPATH) for modelling NET geochemical reactions along a flow path. Version 2.0. US Geological Survey Water-Resources Investigations Report 94-4169.

Schindler, P., Althaus, H., Hofer, F., Minder, W., 1965. Löslichkeitsprodukte von Metalloxiden und hydroxiden: 10. Löslichkeitsprodukte von Zinkoxid, Kupferhydroxoid und Kupferoxid in Abhängigkeit von teilchengrosse und molarer Oberfläche. Ein Beitrag zur Thermodynamik von Grenzflächen fest-flussig. Helv. Chim. Acta 48, 1204.

Schott, J., Berner, R.A., Sjöberg, E.L., 1981. Mechanism of pyroxene and amphibole weathering—I. Experimental studies of iron-free minerals. Geochim. Cosmochim. Acta 45, 2123–2135.

Valsami-Jones, E., Ragnarsdottir, K.V., Putnis, A., Bosbach, D., Kemp, A.J., Cressey, G., 1998. The dissolution of apatite in the presence of metal cations in acidic solutions. Chem. Geol. 151, 215–234.

Velbel, M.A., 1993. Formation of protective surface-layers during silicate mineral weathering under well-leached, oxidizing conditions. Am. Mineral. 78, 405–414.

White, A.F., Brantley, S.L., 1995. Chemical weathering rates of silicate minerals. Reviews in Mineralogy, vol. 31. American Mineralogical Society, Washington, USA, p. 583.

White, A.F., Blum, A.E., Schulz, M.S., Bullen, T.D., Harden, J.W., Peterson, M.L., 1996. Chemical weathering of a soil chronosequence on granitic alluvium: 1. Reaction rates based on

changes in soil mineralogy. Geochim. Cosmochim. Acta 60, 2533–2550.

White, A.F., Bullen, T.D., Vivit, D.V., Schulz, M.S., Clow, D.W., 1999. The role of disseminated calcite in the chemical weathering of granitoid rocks. Geochim. Cosmochim. Acta 63, 1939–1953.

Wilson, M.J., 1987. Clay Mineralogy. Blackie, Glasgow, UK, p. 308.

Zhang, H., Bloom, P.R., Nater, E.A., 1993. Changes in surface area and dissolution rates during hornblende dissolution at pH 4.0. Geochim. Cosmochim. Acta 57, 1681–1689.